Applied Energy 149 (2015) 248–258

Contents lists available at ScienceDirect

Applied Energy

journal homepage: www.elsevier.com/locate/apenergy

Constant heat characterisation and geometrical optimisation of thermoelectric generators

Andrea Montecucco *, Jonathan Siviter, Andrew R. Knox

Thermoelectric Conversion Systems Ltd, UK
School of Engineering, College of Science and Engineering, University of Glasgow, UK

HIGHLIGHTS

- In most waste heat applications at any time the maximum available heat is limited.
- The performance characterisation of TEGs with constant thermal power is presented.
- The influence of the geometrical parameters is analysed.
- The pellets number and geometry are optimised for limited heat systems.
- The efficiency and output power are maximized and the material needed is minimised.

ARTICLE INFO

Article history:
Received 12 August 2014
Received in revised form 20 February 2015
Accepted 23 March 2015
Available online 11 April 2015

Keywords:
Thermoelectric
TEG
Heat transfer
Constant power
Characterisation
Optimization

ABSTRACT

It is well known that for a thermoelectric generator (TEG) in thermal steady-state with constant temperature difference across it the maximum power point is found at half of the open-circuit voltage (or half of the short-circuit current). However, the effective thermal resistance of the TEG changes depending on the current drawn by the load in accordance with the parasitic Peltier effect.

This article analyses the different case in which the input thermal power is constant and the temperature difference across the TEG varies depending on its effective thermal resistance. This situation occurs in most waste heat recovery applications because the available thermal power is at any time limited.

The first part of this article presents the electrical characterisation of TEGs for constant-heat and it investigates the relationship between maximum power point and open-circuit voltage. The second part studies the maximum power that can be produced by TEGs with pellets (or legs) of different size and number, *i.e.* with different packing factors, and of different height. This work provides advice on the optimisation of the pellets geometrical parameters in order to increase the power generated, and consequently the thermodynamic efficiency, and to minimise the quantity of thermoelectric material used, for systems with limited input thermal power.

1. Introduction

Thermoelectric generators (TEGs) are recently being utilised to recover waste heat in a multitude of applications, ranging from low power (sensors [1,2] and battery charging [3]) to medium power (automotive [4,5], stoves [6,7], CHP systems [8], and combined to TPV [9] or PV [10] systems) to high power (heavy-industry [11] and geothermal [12]) because of their reliability, small size and weight, and modular scalability [13].

For a given temperature difference the electrical power delivered by the TEG varies depending on the current drawn by the electrical load connected to its terminals. The TEG can be electrically modelled in thermal steady-state as a voltage source in series with an internal resistance [14,15]. In available literature, to maximise the electrical power extracted from the TEG at any fixed temperature difference the load's impedance should equal the TEG's internal resistance, as stated by the *'maximum power transfer'* theorem [16]. Hence the maximum power point lies at half of the open-circuit voltage V_{OC} or equivalently at half of the short-circuit current I_{SC}.

A characterisation showing the relationship between electrical power, voltage and current for a constant applied temperature difference is an established method to specify the performance of TEG devices. When physically obtaining this characterisation it is necessary to adjust the thermal power through the device because

* Corresponding author.
E-mail address: andrea.montecucco@glasgow.ac.uk (A. Montecucco).

http://dx.doi.org/10.1016/j.apenergy.2015.03.120
0306-2619/

Nomenclature

ΔT	temperature difference (K)
κ	thermal conduction coefficient (W/mK)
l	length (or height) of pellets (or legs) (mm)
L	thickness of the TEG (mm)
K	thermal conductance (W/K)
R	electrical resistance (Ω)
α	seebeck coefficient (μV/K)
a, b, c	parameters for the calculation of V_{OC} (V/K^2, V/K and V, respectively)
d, e, f	parameters for the calculation of R_{int} (Ω/K^2, Ω/K and Ω, respectively)
N	number of pellets in a thermoelctric device
τ	clearance space between pellets (mm)
ω	side length of a pellet (mm)
A	cross-sectional area (mm^2)
V	volume (mm^3)
ϕ	pellets packing (or fill) factor
ZT	dimensionless thermoelectric figure of merit

a change in electrical load varies the effective thermal conductance of the TEG due to the Peltier effect [17]. This method of characterisation is referred to as constant temperature operation, and its use effectively masks the complex and subtle device response to variable load current. The internal resistance (R_{int}) is the inverse slope of the V-I line obtained from this electrical characterisation, and its absolute value is dependent on the average temperature at which the TEG is operating. When the TEG is operated to the left of the maximum power point as shown in Fig. 1, reduced current flows through the TEG and the effective thermal conductivity of the TEG (which depends also on the current flow, due to the parasitic Peltier effect) decreases. Under this condition the thermal energy conducted via the TEG is less than that at the maximum power point and hence a lower thermal load is imposed on the overall system. This is advantageous in most circumstances since it leads to increased thermal efficiency of the system. When the TEG is operated to the right of the maximum power point the thermal conductivity increases and the thermal energy conducted via the TEG is greater than that which flows at the maximum power point. Operation in the region to the right on Fig. 1 leads to a reduced thermal efficiency of the system. For the module data (product code: GM250-449-10-12 by *European Thermodynamics Ltd.*) shown in Fig. 1, the maximum power is approximately 13.2 W with a corresponding output voltage of 16.5 V (being half of the open-circuit voltage of 33 V).

In most practical applications, however, and especially in automotive exhaust gas energy recovery systems, TEGs are subject to limited thermal input energy rather than to a constant temperature difference. This is referred to as "constant heat" operation. Kumar et al. [18] observed strong variations of the electrical power generation with the exhaust gas flow rate and temperature, *i.e.* the input thermal power. The available thermal energy may change with time, but its rate of variation will be orders of magnitude slower than the TEGs electrical response [19]. In considering the constant heat condition, changing from open-circuit to at-load operation results in a smaller temperature difference across the device, due to its greater effective thermal conductivity. The change of temperature difference after a transient that could last for several seconds thus leads the device to produce lower electrical power.

Mayer and Ram [20] firstly noticed that when the temperature gradient across the TEG is not constant the optimum current is lower than that required for constant temperature systems. Moreover, they found that this optimum load also differs from the load that maximises efficiency in constant temperature systems. They also provided guidance on the optimisation of the pellet length per unit area. Similar results about optimum load condition are reported by Gomez et al. [21]. They compared a model in which the temperatures are constant with a model in which the temperatures on the sides of the device vary depending on the load, while the ambient temperature and the hot-source temperature (separated from the TEG by thermal resistances) are constant. We proposed similar results about the influence of the load on the temperature profile -with a different analytical solution that can also simulate time transients- in [22].

Yazawa and Shakouri [23] optimised the thermoelectric device design together with its heat source and heat sink at constant temperatures. They concluded that the optimum operating load is when $R_{load} = R_{int}\sqrt{1+ZT}$, where R_{int} is the internal resistance and ZT is the figure of merit of the thermoelectric device. They also suggested that using low fill (or *packing*) factors could increase the electrical power output per unit mass. McCarty [24] confirmed Yazawa's result and provided equations to calculate the optimum number of couples and pellets length-to-area ratio as functions of the total thermal resistance of the system and for fixed electrical load, hot-side temperature and material properties. However, the value of $ZT = \sigma\alpha^2 T_{AVG}/\kappa$ depends on the electrical conductivity (σ), the Seebeck coefficient (α), the thermal conductivity (κ) and the average temperature of the semiconductor material, T_{AVG} (in degrees Kelvin), therefore it is difficult to calculate its correct value before knowing the effective operating temperatures. Nemir and Beck [25] explained that the maximum efficiency in constant temperature is dependent only on the temperatures and ZT, but not on the particular values of σ, κ and α. They also investigate the influence of thermal interfaces but they do not analyse the variations on thermal power through the TEG. Apertet et al. [26] complemented this analysis.

The previous literature reported here ([20,21,23–26]) effectively considered a system in which the thermal input power varies depending on the load, because the hot-source temperature and cold-source (often ambient) temperature are maintained constant (ideal temperature sources). For such reason maximum power and maximum efficiency are at different points. On the contrary, in constant heat systems the point that maximises the electrical power output also guarantees maximum efficiency, as introduced by Wang et al. [27] and further described in this article.

Despite high ZT values recently claimed by thermoelectric material scientists, there is not much literature focused on improving the thermoelectric device design and architecture. Rezania et al. [28] focused on the single thermoelectric element to optimise the ratio of the cross-sectional areas of the *p*- and *n*-semiconductor pellets; they concluded that maximum power generation occurs when the area of the *n*-pellet is smaller than that of the *p*-pellet, due to lower electrical resistance and higher thermal conductivity of the *n*-type material considered. Lee [29] focused on the design of thermoelectric devices in conjunction with the heat sinks performance, asserting that there is an optimal ratio of system thermal conductivities to provide maximum power output. Jang and Tsai [30] and Favarel et al. [31] modify the spacing between TEG modules (or the occupancy rate) placed on a heat exchanger of fixed geometry to maximise the power output depending on the available thermal power. Kajihara [32] presented an analysis of the influence of legs' width, height, gap (clearance) and number

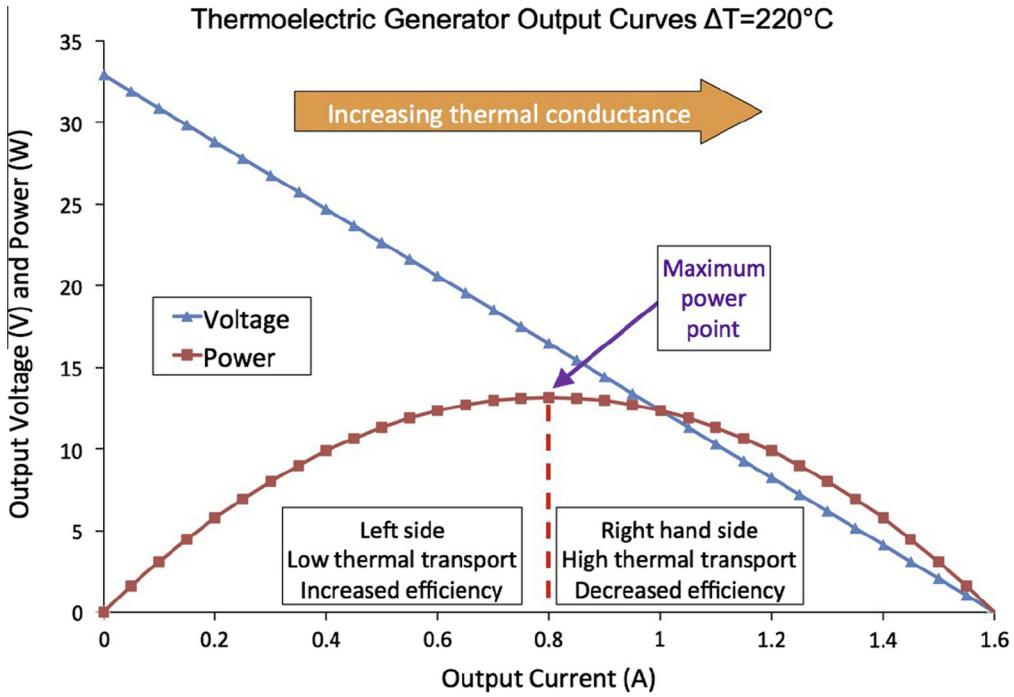

Fig. 1. Electrical characterisation (V-I and P-I curves) of the thermoelectric device *GM250-449-10-12* by *European Thermodynamics Ltd*.

for a constant temperature difference. Wide pellets with small gap between them lead to high power generation but also require great amounts of heat through them and the author also considers manufacturing constraints.

This work analyses the performance of a TEG device under steady-state thermal conditions of constant heat through it (as opposed to constant temperature difference), for varying number and size (both width and height) of pellets, and clearance space between them. This study is independent from the effect of the heat exchangers in contact with the TEG, and the associated thermal contact resistances. The design of the heat exchangers can be undertaken independently.

This article firstly presents a steady-state theoretical analysis of the power balance in constant heat TEG systems, which is used to provide the electrical characterisation (V-vs-I and P-vs-I), which has not been previously presented in literature. The optimum operating point is located between the open-circuit and the maximum power point of "constant temperature" systems. In fact this load point, which is characterised by a higher output voltage compared to the maximum power point, has a reduced Peltier effect which results in a greater temperature difference across the device and consequently yields higher electrical power production and greater system efficiency.

This article then provides a detailed analysis of the influence on the thermoelectric performance of the *fill* (or *packing*) factor, which is related to the number and cross-sectional area of the pellets (or legs), and the clearance space between them. Firstly, a comparison is provided for commercial TEG devices with same overall surface area but different number of pellets of dissimilar size, which often results in different fill factors. Secondly, a simulation tool is used to optimise the number of pellets and clearance space between them depending on the available heat power in constant heat TEG systems. Different combinations of pellets number and clearance space result in optimum performance, with the same pellets packing factor in all instances.

The simulation tool is further improved to optimise the TEG device geometry modifying both the pellets packing factor and height (or thickness). The resulting simulation model provides an optimisation tool to design the geometrical parameters of the TEG device in order to increase power production and efficiency while minimising the quantity of thermoelectric material used only by acting on the physical architecture of the TEG pellets.

The results provided offer interesting insights on the breakdown of powers due to the thermoelectric effects and assist in the design of the TEG device depending on its intended use and available thermal power.

2. Constant-heat characterisation of TEGs

First consider a TEG sandwiched between a cold side at temperature T_C and a hot side at temperature T_H, both of which can vary their temperature. As explained by Min and Yatim [17], the effective thermal conductance K_{var} of the TEG varies depending on the amount of current drawn from it, and it can be calculated as

$$K_{var} = \frac{Q_H}{T_H - T_C} \tag{1}$$

where Q_H is the thermal power flowing through the TEG, considered constant throughout this discussion. Moving from open-circuit to at-load, K_{var} increases and the temperature difference decreases as T_C increases and T_H decreases. If T_C is maintained at a constant temperature then T_H must decrease by the deviation corrected for in T_C to keep $\Delta T = T_H - T_C$ as previously. Hence we can set T_C as a constant without significant loss of accuracy; the only small difference is represented by the fact that the thermal conductivity, κ, and the electrical resistivity, ρ, slightly vary with the average temperature of the device, but in this case the average temperature is almost unchanged. Not only this assumption allows to maintain the thermal power constant despite changes in T_H, but this assumption is also realistic: in most TEG systems the cold side temperature remains almost constant with relatively small changes in thermal power flowing into the cold side. Also, this analysis allows to neglect the effect of the contact resistances, because the temperature difference can vary, depending on the effective TEG thermal resistance and the thermal power flowing through it, with reference to the constant T_C.

The steady-state thermal input power to the hot junction is derived from the steady-state solution of the one-dimensional heat conduction equation for solids with internal energy generation, assuming constant temperatures at the hot and cold side as boundary conditions [15]. In this analysis the Thomson effect is not considered due to its negligible effect [33,34]:

$$Q_H = \frac{\kappa A \Delta T}{L} + \alpha T_H I - \frac{1}{2} R_{int} I^2 \quad (2)$$

where κ is the heat conduction coefficient, A is the area and L the thickness of the TEG, ΔT is the temperature gradient, α is the Seebeck coefficient and R_{int} is the overall internal resistance of the device. In Eq. (2) both R_{int} and α vary with ΔT. It is possible to express their variation with ΔT using a 2nd-order polynomial equation, so that the load voltage can be written as a function of I_{load} and ΔT:

$$V_{load} = (a\Delta T^2 + b\Delta T + c) - (d\Delta T^2 + e\Delta T + f) I_{load} \quad (3)$$

where a, b, c, d, e and f are constant coefficients, different for each TEG and obtained from experimental data [35]. They are listed in Table 1. Using $\alpha = a\Delta T + b + c/\Delta T$ and $R_{int} = d\Delta T^2 + e\Delta T + f$ in Eq. (2) results in:

$$Q_H = K(T_H - T_C) + \frac{a(T_H - T_C)^2 + b(T_H - T_C) + c}{T_H - T_C} T_H I - \frac{d(T_H - T_C)^2 + e(T_H - T_C) + f}{2} I^2 \quad (4)$$

where $K = \kappa A/L$ is the thermal conductance of the TEG in [W/K] at open-circuit. The second term on the right side of Eq. (4) considers the Seebeck coefficient for the whole device as $V_{OC}/\Delta T$; even if α should be divided by the number of pellets, it needs to be multiplied again by the same number for the calculation of the Peltier power.

Eq. (4) in the variable T_H has three real solutions, which can be easily calculated by *Matlab*[1] and the correct solution thus identified. Using Eq. (4) it is possible to obtain the variation of the steady-state temperature difference across the TEG versus the load current, as it will be shown in Fig. 2. A graph reporting the variation in temperature difference versus load change was presented in [17] for different values of the figure of merit Z, considered constant over the temperature range.

It is trivial to calculate the steady-state temperature difference at open-circuit ΔT_0, at which the TEG is producing the open-circuit voltage V_{OC_0}. If there were no changes in temperature difference due to the Peltier effect and Joule heating then the maximum power point would be found at $V_{load} = V_{OC_0}/2$. In reality after drawing current from the TEG the temperature difference decreases exponentially to the steady-state value. Due to the long thermal time constant of a typical thermoelectric system, it may take several seconds to complete at least 90% of the transition.

A program was written in *Matlab* in order to find the value of I that leads to the maximum power production: starting from open-circuit and gradually increasing the load current I the corresponding steady-state temperature difference is calculated solving Eq. (4), and the output power is then obtained by multiplying Eq. (3) by I. A single TEG with the thermal and electrical characteristic of the device GM250-127-14-10[2] (characterised in [35]) was considered for this analysis. The value of thermal conductivity at open-circuit is $\kappa_{OC} = 1.5$ W/mK, $T_C = 25$ °C and $Q_H = 156$ W. The thermal conductivity is considered constant because it is difficult to obtain confident measurements of it at different temperatures. Its variation might slightly affect the results presented here.

[1] www.mathworks.com.

[2] by European Thermodynamics Ltd (www.europeanthermodynamics.com/index.php/products/thermal/thermoelectrics/power-generation/gm250.html).

Table 1
The a, b, c, d, e, f coefficients used in the simulations.

V_{OC} (V)			R_{int} (Ω)		
a (V/K^2)	b (V/K)	c (V)	d (Ω/K^2)	e (Ω/K)	f (Ω)
$-7 \cdot 10^{-5}$	0.0639	−0.8536	$-9 \cdot 10^{-6}$	0.0062	1.1972

Fig. 2 shows the resulting electrical characterisation computed by *Matlab* for constant thermal power input, in steady-state; for each load point (blue line), the green line plots the temperature difference (on the secondary y-axis) and the red line the produced power. It can be noted that the temperature difference decreases significantly with increasing current loads due to an increase in heat pumped from the hot to the cold side. When going from open-circuit to maximum power the temperature difference drops 40 °C from $\Delta T_{OC} = 195$ °C to $\Delta T_{MP} = 155$ °C, and the ΔT at short-circuit is 124 °C. The maximum power is obtained for $V_{MP} = 4.32$ V which is almost half of the initial open-circuit steady-state voltage $V_{OC_{init}} = 8.95$ V, which is the highest voltage that the system can produce. This is due to the slight bend in the voltage line which is in turn due to the not-exactly linear variation of the Seebeck effect with the temperature difference (see Eq. (3)). Hence it is found that the "real" MPP is around 0.483 times the steady-state open-circuit voltage, $V_{OC_{init}}$, and that this relationship holds similarly for other TEG geometries.

In practical TEG systems for waste heat recovery maximum power point tracking (MPPT) converters are employed to maximise the power produced by the TEGs at any time. Due to the fast frequency response of the electronic converters, both the fractional open-circuit algorithm [36] as well as hill climbing algorithms [37,38] set the operating load at half of the open-circuit voltage, which is the optimum operating point of the constant temperature difference electrical characterisation.

The next aim of the program is to compare the value of maximum power found before to the one that would be set if the load voltage was to be continuously adjusted to half of the instantaneously resulting open-circuit voltage. This does not mean that an open-circuit condition is applied to the load (in which case the temperature difference would go back to $\Delta T_{OC} = 195$ °C, corresponding to $V_{OC_{init}} = 8.95$ V, after a certain transient time). The "instantaneous" V_{OC} corresponds to the voltage that would be established immediately after a sudden disconnection of the load, and it is always smaller than $V_{OC_{init}} = 8.95$ V. The program uses a recursive loop to adjust the operating voltage V_{load} at half of the V_{OC} calculated in the previous iteration. The recursive operation is needed because when a new voltage is applied the current changes accordingly and so does the temperature difference. A new V_{OC} is established and V_{load} must be updated again. The program is considered to have achieved convergence when the difference between V_{load} and $V_{OC}/2$ is less than 1 mV. This V_{OC} is marked by a magenta circle on the primary y-axis of Fig. 2 (7.14 V), while the open-circuit voltage related to the maximum power point is marked by a black circle (7.39 V). As a result of this analysis the load chosen ($I_{HV} = 1.86$ A) is greater than $I_{MP} = 1.58$ A, leading to a smaller $\Delta T = 149.6$ °C and a power produced of 6.62 W, which is 2.9% smaller than $P_{MP} = 6.82$ W.

Summarising these results, the output voltage that leads to maximum power production in case of fixed thermal input power is greater than $V_{OC}/2$ but correspondent to almost half of $V_{OC_{init}}$. The smaller current drawn reduces the Peltier effect, thus resulting in a higher temperature difference across the device and a corresponding higher power produced.

It is very important to re-iterate that these results are calculated for the thermal steady-state under constant thermal input power,

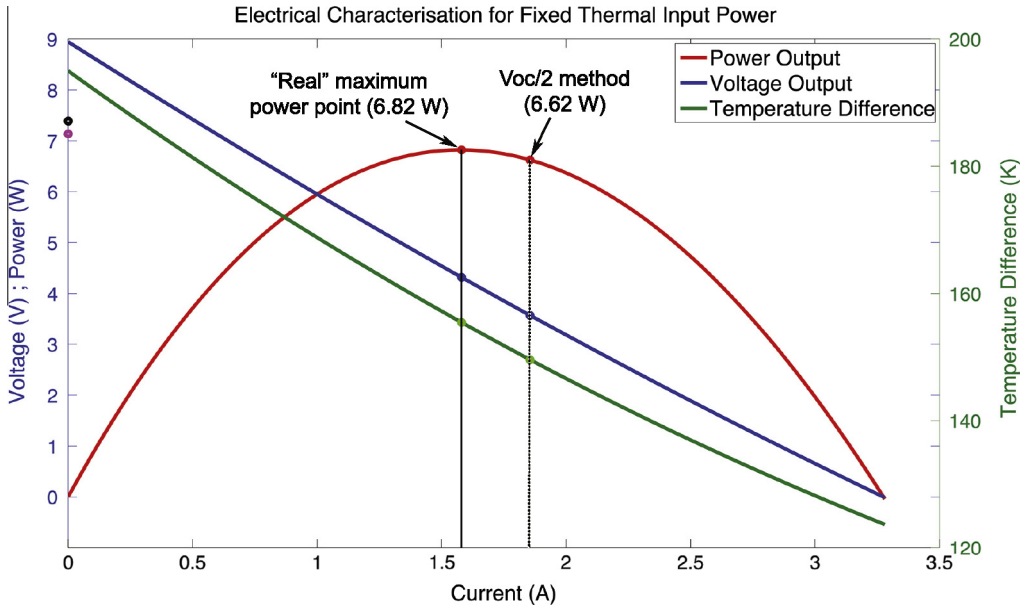

Fig. 2. Electrical characterisation of a TEG with fixed thermal input power $Q_H = 156$ W. V-I line in blue, P-I curve in red, ΔT-I line in green. Point of maximum power production: $V_{MP} = 4.32$ V,$I_{MP} = 1.58$ A,$\Delta T = 155$ °C with $V_{OC} = 7.39$ V (black circle). Point set by continuously adjusting $V = V_{OC}/2 : V_{HV} = 3.56$ V,$I_{HV} = 1.86$ A,$\Delta T = 150$ °C, with $V_{OC} = 7.14$ V (magenta circle). (For interpretation of the references to colour in this figure legend, the reader is referred to the web version of this article.)

which is usually reached after several minutes. In some thermoelectric power generation applications the thermal input power varies fairly rapidly with time, *e.g.*, exhaust gas mass flow and temperature. When varying the electrical operating point from $V_{OC}/2$ to V_{MP}, the change in hot-side temperature is quite slow – dominated by the thermal time constants of the system – so that the immediate change in power production could be negligible, if not negative. However, for certain driving conditions, or in other applications with slower variations of thermal input power, setting the load at V_{MP} instead of $V_{OC}/2$ could prove beneficial.

3. Effect of the pellets packing factor

This section studies the electrical performance and thermal behaviour exhibited by commercial TEG devices made of different number of pellets (or legs) with dissimilar sizes, but with the same overall size and height.

Firstly, assume that two TEGs can hypothetically be produced without clearance space between pellets. If these two devices are made of the same quantity of thermoelectric material but have pellets of dissimilar size (and same height), they will produce the same amount of electrical power and have the same thermal behaviour; what changes is the current and voltage rating. In practice it is impossible to manufacture two thermoelectric devices like those just described. The necessary clearance space between pellets usually leads to different *packing* (or *fill*) factors for devices of equal overall dimensions but with different pellet sizes. The clearance space, labelled hereafter τ, usually ranges from 0.8 to 1.2 mm; as a consequence, commercial devices with wider pellets contain a greater quantity of thermoelectric material (considering constant the pellets' height). In a square thermoelectric device with total surface area A comprising of N square pellets, the side length ω of each pellet can be calculated as

$$\omega = \frac{\sqrt{A} - \sqrt{N+2}\,\tau}{\sqrt{N+2}} \tag{5}$$

where $N+2$ is used because two locations without pellets are occupied by the two electrical wires. In Eq. (5) it was considered the same number of pellets and clearance spaces in each side of the device (half clearance space at each corner).

The packing factor, ϕ, is defined as the ratio of surface area of thermoelectric material ($N\omega^2$) over the total surface area (A) of the module and obtained from

$$\phi = \frac{N\left[A + (N+2)\,\tau^2 - 2\sqrt{A}\sqrt{N+2}\,\tau\right]}{A(N+2)} \tag{6}$$

In order to compare the thermoelectric performance of TEGs with the same A but different ω, the parameters used in Section 2 are normalised to the mechanical parameters of device GM250-127-14-10 ($N_{norm} = 254, A_{norm} = 40 \times 40$ mm^2, $\omega_{norm} = 1.4$ mm) and then adapted to a TEG device with different number of pellets N and side length ω. The same height of pellets is used. This procedure is described next:

- the pellet side length w is calculated from Eq. (5),
- a, b, c (related to V_{OC}) are scaled by $N/254$,
- d, e, f (related to R_{int}) are scaled by $1.4^2 N/254\omega^2$,
- the open-circuit thermal conductance of the pellets, $K_{pellets}$, varies linearly with the packing factor, hence it is scaled by $\frac{\omega^2 N}{1.4^2 \cdot 254}$.

The parameters d, e, f are obtained experimentally therefore R_{int} includes the effects of the electrical contact resistances (copper tabs). The scaling of R_{int} depends on the number of pellets to which the electrical contact resistances are related, whence scaled appropriately. The thickness of the Alumina ceramic substrate is considered constant at 1 mm with thermal conduction coefficient $\kappa_{ceramic} = 36$ W/mK. The thermal resistance of the thin copper contacts is considered negligible, therefore the total thermal conductivity of the TEG device is calculated as $1/K_{TEG} = 2/K_{ceramic} + 1/K_{pellets}$.

Table 2 presents the parameters of the three TEGs considered in this section: the first is the TEG analysed in Section 2 ($N = 254, \tau = 1.1$ mm), the second is a TEG with $N = 482$ and $\tau = 0.8$ mm (GM250-241-10-12 by *European Thermodynamics Ltd*), and the third is a TEG with $N = 110$ and $\tau = 1$ mm (equivalent

Table 2
Geometrical, thermal and electrical parameters of the three TEG devices considered.

	N	τ (mm)	w (mm)	ϕ	K (W/K)	R_{int} (Ω)
TEG 1	254	1.1	1.4	0.31	0.8	1.94
TEG 2	482	0.8	1	0.31	0.8	6.97
TEG 3	110	1	2.8	0.53	1.37	0.184

to GM250-31-28-12 by *European Thermodynamics Ltd* scaled from 30×30 mm^2 to 40×40 mm^2 for comparison with the other two devices). A comparison of the values of R_{int} and V_{OC} obtained with this procedure to experimental results shows a maximum error of 6.94%. This can be due to different performance of the Bi_2Te_3 used, electrical and thermal contact resistances, manufacturing tolerances or test accuracy.

Table 3 presents the three sets of results related to the TEGs used (Table 2) and obtained maintaining constant $Q_H = 156$ W and $T_C = 25$ °C. The first two devices have the same packing factor ϕ, which results in the same values for thermal conductivity K and temperature difference ΔT across the device. The maximum electrical power produced for constant thermal power through the device, Peltier power and Joule power are also equivalent. The third device, characterised by a packing factor 1.7 times greater, demonstrates worse performance because its higher K leads to a considerably lower ΔT and consequently lower maximum electrical power (1.5 times smaller). As a comparison with the results presented in Section 2 (for the first TEG), in which the difference ΔP_{out} between maximum power and power set by the half open-circuit voltage method was 2.9%, for the third TEG this difference rises to 4.6%. This difference is not related to the particular geometry of the TEG, but to the temperature difference and it increases when the temperature difference decreases. In other words ΔP_{out} decreases at greater ΔT, which is when the power output and the thermal-to-electrical efficiency increase.

It was already introduced in Section 2 that the maximum power is extracted for a voltage greater than $V_{OC}/2$. Consider the at-load voltage as a fraction of the "instantaneous" open-circuit voltage:

$$V = \beta V_{OC} \tag{7}$$

In Table 3 $\beta = 0.585$ for the first two TEGs and $\beta = 0.608$ for the third TEG. Running the same simulation for other values of Q_H it is noteworthy to discover that this relationship depends on ΔT : $\beta \approx 0.62$ at $\Delta T = 50$ °C and it varies linearly towards $\beta \approx 0.55$ at $\Delta T = 275$ °C. This variation in the optimum value for β might be related to the variation of the thermoelectric coefficients with the temperature difference.

The power pumped from the hot side due to the Peltier effect (P_{Pelt}) remains almost constant, but this effect is further investigated in Section 4. For all devices analysed $P_{Pelt} + K\Delta T - P_{Joule}$ is equal to $Q_H = 156$ W (note that $P_{Joule} = 0.5RI^2$).

Table 4 compares the results obtained in this analysis with previous literature. For all three TEGs the optimum load is different from the one proposed by Yazawa and McCarty ($R_{lit} = R_{int}\sqrt{1+ZT}$) [23,24]. The difference is around 11% for the first two TEGs and 17% for the third one. However, it must be highlighted that these results cannot be used for a direct comparison because they are obtained with constant heat flux but varying temperature difference (as opposed to constant temperature difference and varying heat input as done in literature). ZT is calculated considering the variation of both the Seebeck coefficient,α, and the electrical conductivity, σ, with the temperature difference (from Table 3 and Eq. (3)), while the thermal conduction coefficient, κ, is maintained constant at 1.5 W/mK.

Table 4
Comparison of results from this work with literature: $R_{lit} = R_{int}\sqrt{1+ZT}$ [23], $m_{\Delta T} = \frac{\Delta T_{OC}}{\Delta T_{SC}}$ [17].

	ZT	R_{load}	R_{lit}	ΔT_{OC}	ΔT_{SC}	$m_{\Delta T\ here}$	$m_{\Delta T\ lit}$
TEG 1	0.585	2.73	2.45	195.0	123.8	1.57	1.59
TEG 2	0.585	9.88	8.77	194.3	123.5	1.57	1.59
TEG 3	0.633	0.29	0.24	116.5	73.2	1.59	1.63

The ratio between the open-circuit and short-circuit temperature differences, $m_{\Delta T}$, agrees with the one proposed by Min [17], $m_{\Delta T} = 1 + ZT$, in all cases.

The differences evinced from Table 3 highlight the great influence of the packing factor on the performance of commercial thermoelectric devices. In particular its influence on the thermal conductivity makes one device suited for a particular application, depending on the available thermal energy, to establish a high temperature difference, or to protect the TEG device from excessive temperatures.

4. Optimisation of the pellets packing factor

This section presents an expansion of the analysis presented in Section 3 that can be used to design the geometry of the pellets and the clearance space between them, for any preferred thermal operating point and for constant pellets thickness (or height). The same code used in the previous sections is inserted in a nested *for* loop relative to the number of pellets N and the clearance space τ to calculate the geometry of TEG devices that leads to maximum power generation in conditions of constant thermal power flowing through the device. For each pair of values of N and τ the algorithm calculates the pellet side length ω and the packing factor ϕ from Eqs. (5) and (6), respectively. The algorithm rejects values of ω smaller than a certain threshold ($\omega_{min} = 0.75$ mm), due to practical manufacturing constrains. The impact of solder contacts on the electrical resistance is included in this study because the values of the parameters d, e, f (in Eq. (3) and Table 1) are obtained experimentally, thus clearly including the electrical contact resistances. The algorithm excludes data points that would establish hot side temperatures greater than $T_{max} = 300$ °C for Bi_2Te_3. The algorithm finally stores all the values of interest in arrays and plots the surfaces related to the x and y axes of τ and N, respectively.

A simulation was computed varying the number of pellets between 50 and 600 and the clearance space between 0.6 and 2.4 mm, for $Q_H = 156$ W and $T_C = 25$ °C. The resulting surfaces for the maximum electrical power output, temperature difference, Peltier power, pellets side length, fill factor and volume of thermoelectric material needed are shown in Fig. 3 from the z-axis; the granularity is due to the discrete values used for N and τ. It can

Table 3
Simulation results to compare the effect of pellets' dimensions and packing factor on the thermoelectric performance when considering a system with constant thermal input power.

	ΔT (K)	α (μV/K)	I (A)	V (V)	V_{OC} (V)	P_{elec} (W)	ΔP_{out} (%)	P_{Pelt} (W)	P_{Joule} (W)
TEG 1	155.5	187	1.58	4.32	7.39	6.82	2.90	34.1	2.4
TEG 2	155.0	187	0.83	8.2	14.0	6.81	2.92	33.9	2.4
TEG 3	92.8	190	4.08	1.18	1.94	4.80	4.59	33.3	1.6

be seen that there are several combinations of N and τ that lead to almost identical performance. Fig. 3c shows that the pellets side length progressively decreases for greater N and τ. In each plot of Fig. 3 the points related to the TEGs of Table 2; the point that provides optimum performance is also marked ($N = 180, \tau = 1.7$ mm,$\omega = 1.27$ mm).

Fig. 3b shows that the maximum allowed temperature difference of 275 °C can be reached with numerous combinations of N and τ, all correspondent to the same values of fill factor ($\phi = 0.18$), as per Fig. 3d, and thermal conductivity ($K_{TEG} = 0.47$ W/K). The optimum point produces $P_{max} = 8.34$ W at $V = 4.46$ V, $I = 1.87$ A.

The Peltier power is similar for all TEGs and it seems to follow the variation of the Seebeck coefficient with temperature, with peak values at temperatures lower than T_{max} for Bi_2Te_3. The power due to the Joule effect increases when power generation is greater.

It can be seen from Fig. 3a that the commercial TEG with large pellets produces almost half of what could potentially be extracted in this constant Q_H situation. This is due to its high packing factor ($\phi = 0.53$), resulting from the use of large pellets ($\omega = 2.8$ mm) and clearance space of similar value to that of the other two commercial TEGs ($\tau = 1$ mm) that produce around 6.8 W. However, the results presented in this section suggest that high power can still be obtained using big pellets provided that the clearance space between them is increases substantially, *e.g.*, $N = 80$, $\omega = 2$ mm, $\tau = 2.4$ mm, in order to keep the packing factor ϕ (and consequently the thermal conductivity K) down. However, this solution would lead to low voltage/high current ratings for the device, which is usually more difficult to deal with in the power electronics conditioning system. The volume of necessary thermoelectric material remains constant for same values of packing factor.

Fig. 3a shows that an optimisation of the pellets geometry could improve power production from the analysed constant heat condition of $Q_H = 156$ W from 6.8 W to 8.3 W, which corresponds to an increment of almost 20%.

The thermal to electrical efficiency of thermoelectric generators is calculated as

$$\eta = \frac{P_{elec}}{Q_H} \tag{8}$$

and Q_H is constant, therefore an increase in electrical power output directly improves η. In this case η would increase by around one percentage from 4.36% to 5.34%.

Longer pellets reduce the thermal conductivity of the device, thus improving the efficiency, but at the same time they increase the electrical resistance, hence the current output decreases because the open-circuit voltage remains the same. The effect of pellet length (or thickness) is analysed in Section 5.

5. Optimisation of the pellets geometry

The aim of this section is to investigate the effect on performance and material cost of a varying pellets thickness (or height). Section 4 highlighted that for a constant pellets thickness (or height) a certain pellets packing factor leads to same performance, irrespective of the values of N and τ. Therefore the simulation tool is modified to analyse performance as a function of the pellets packing factor, ϕ, and height, h. For this analysis the results are

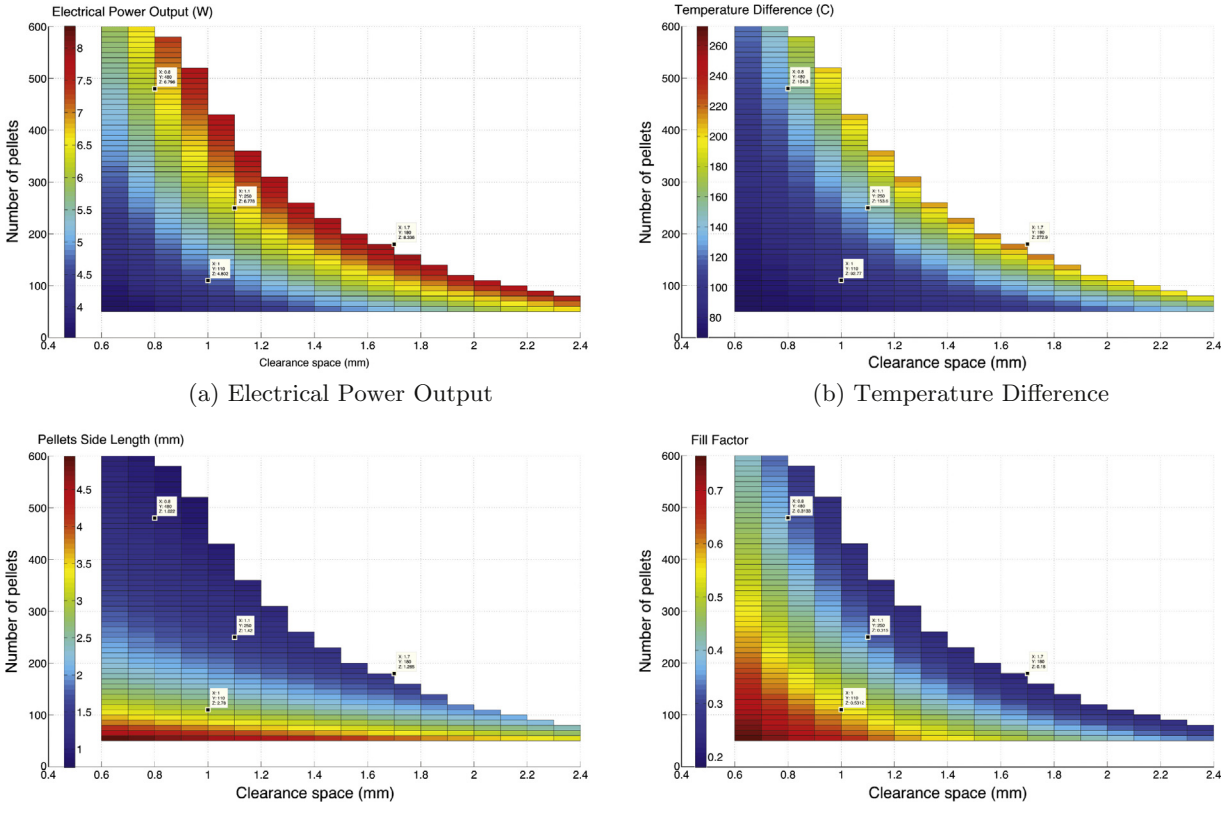

(a) Electrical Power Output

(b) Temperature Difference

(c) Pellets Side Length

(d) Pellets Fill Factor

Fig. 3. Surface plots (viewed from the z-axis) as functions of the number of pellets (y-axis) and the clearance space (x-axis). Note that the colours selected by *Matlab* for each box are related to the values of the left corners. (For interpretation of the references to colour in this figure legend, the reader is referred to the web version of this article.)

obtained using $N = 250, Q_H = 156$ W, $\kappa = 1.5$ W/mK, $T_C = 25$ °C and h is varied between 0.6 and 2.4 mm.

Fig. 4 shows the resulting surfaces, viewed from the z-axis, of the electrical power output, temperature difference, internal resistance and thermal conductance. It is easy to note that multiple combinations of pellets height and packing factor lead to maximum performance, and the data cursors mark the calculated maximum power point for reference. However, a noteworthy result can be obtained by calculating the volume of thermoelectric material needed for each pellets design. This is plotted in Fig. 5, where it can be seen that the volume is minimum for short pellets characterised by a small fill factor, and maximum when using long pellets with high packing factor. The difference between minimum and maximum volumes leading to identical performance is almost one order of magnitude, which constitutes a significant difference.

This simulation is run also for different values of input thermal power: $Q_H = 50, 100, 150, 200, 250$ W. Some important results are listed in Table 5. In all cases, the simulation tool aims at finding the TEG design that establishes a temperature difference of 275 °C across the TEG, therefore the open-circuit voltage, which depends on N and α, is always $V_{OC} = 11.2$ V. Confirming the results of Section 2, the load voltage for maximum power is always at $V_{MP} = 6.2\ V$.

The thermal-to-electrical efficiency and figure of merit are in all cases $\eta = 5.35\%$ and $ZT = 0.455$, respectively. The electrical power output, P_{out}, increases linearly with Q_H because η is constant: $P_{out} = \eta Q_H$. The same trend is exhibited by the current produced at the maximum power point: $I_{MP} = P_{out}/V_{MP}$.

It is very important to note from Table 5 that the optimum TEG thermal conductance varies linearly with Q_H. This does not mean that the optimum K can simply be calculated by $Q_H/\Delta T$. In fact, this occurs because the heat removed from the hot side by the Peltier effect is always the same fixed percentage of Q_H, equal to 20.2% in all cases. The same occurs for the Joule power, whose percentage of Q_H is 2.15%. This result is noteworthy, because it allows to calculate the optimum thermal conductance to achieve a desired temperature difference ΔT by

$$K_{opt} = \frac{Q_H - 0.202 \cdot Q_H + 0.0215 \cdot Q_H}{\Delta T} \approx \frac{0.82 \cdot Q_H}{\Delta T} \tag{9}$$

The efficiency obtained ($\eta = 5.35\%$) seems to agree with the value proposed by Min [39]:

$$\eta_{max} = \frac{\Delta T}{T_H} \frac{\sqrt{1+ZT}-1}{\sqrt{1+ZT}+T_C/T_H} = 5.7\% \tag{10}$$

Contrary to the comparison results obtained in Section 3 (Table 4), in Table 5 $R_{lit} = R_{int}\sqrt{1+ZT} \approx R_{load}$, with a difference of only 2.5%. This could be determined by the fact that the results in this section are obtained for optimised values at maximum allowed temperature difference. The difference then widens for less optimised pellets and lower temperatures.

Similar result trends were obtained also using $N = 100$ and $N = 400$.

Summarising the results achieved in this section, the output power and efficiency do not depend on the pellets geometry and can be obtained by a multitude of combinations of the TEG geometrical parameters (mainly pellets number, size and clearance space between them). However, the quantity of thermoelectric material can be minimised when using shorter pellets with small fill factor.

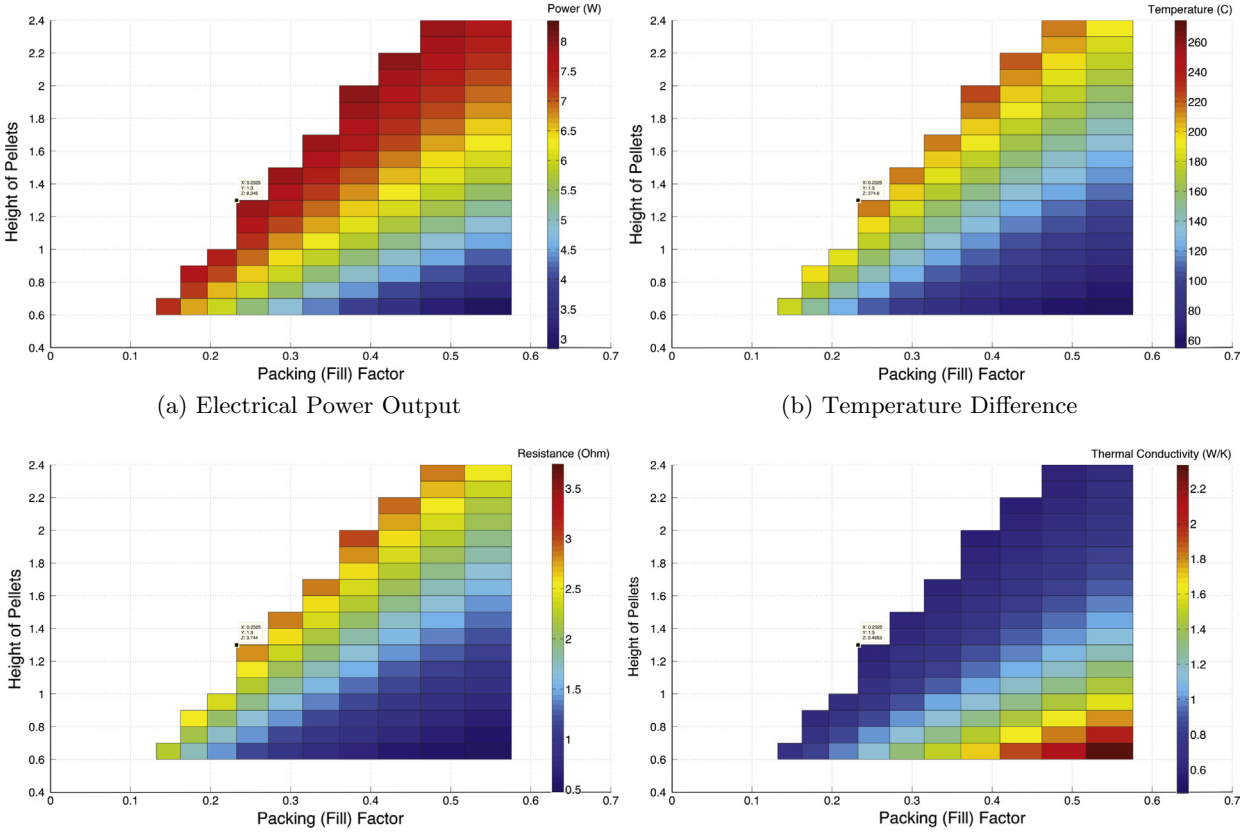

(a) Electrical Power Output

(b) Temperature Difference

(c) TEG Internal Resistance

(d) TEG Thermal Conductance

Fig. 4. Surface plots (viewed from the z-axis) as functions of the pellets fill factor (y-axis) and height (x-axis), for $Q_H = 156$ W.

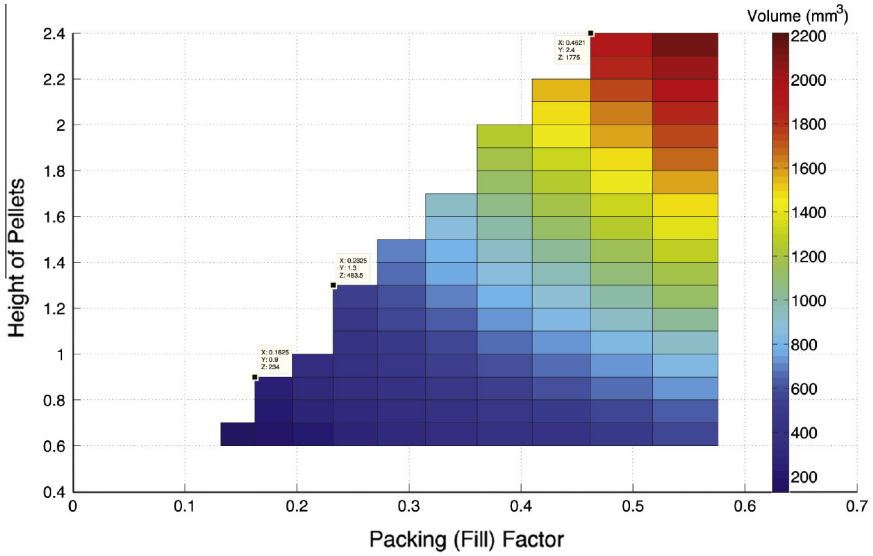

Fig. 5. Volume of thermoelectric material required to produce a TEG with $N = 250$ pellets of varying dimensions, as function of the pellets fill factor (y-axis) and height (x-axis), for $Q_H = 156\,W$.

Table 5
Optimisation of pellets packing factor and length of a TEG with $N = 250$ pellets, for five values of constant thermal input power ($Q_H = 50, 100, 150, 200, 250$ W).

Q_H	R_{int}	K	R_{load}	R_{lit}
50	11.63	0.15	14.30	14.03
100	5.80	0.30	7.18	7.00
150	3.90	0.45	4.82	4.70
200	2.90	0.60	3.59	3.49
250	2.32	0.74	2.86	2.79

6. Discussion of results

The first part of this work presented the thermal and electrical characterisation of TEGs under steady-state constant heat conditions (Fig. 2). The relationships between the optimum operating voltage and both the initial and the instantaneous open-circuit voltages are provided in Sections 2 and 3.

The second part offered an innovative solution to calculate the optimum thermal conductance (Eq. (9)) to obtain a desired temperature difference across the TEG, for a constant heat input. Also, the variation trend of thermoelectric material required for any combination of pellets height and fill factor was plotted in Fig. 5 to show that optimum values of the pellets geometrical parameters can be selected to minimise the thermoelectric material cost.

In this study the thermal contact resistances, as well as the thermal resistance of the copper tabs and solder, were not considered. The variation of thermal conductivity with temperature was not considered due to the difficulty in obtaining precise measurements of it. Nonetheless, in the results presented here the temperature difference between points around the optimum ones does not vary significantly, hence the variation of thermal conductivity should not affect the results. For what concerns the constant power characterisation, the temperature difference changes by around 70 °C thus not leading to great variation in thermal conductivity.

The electrical resistance of the copper tabs and solder was considered because the experimental values used in the simulations implicitly include this resistance. This work included the variation of both the Seebeck coefficient and the electrical resistivity with the temperature as per Eq. (3), while the open-circuit thermal conductivity has been considered constant. It must be noted that the results presented in this article are related to the experimental performance of the device tested. Nonetheless the results can be extended to similar commercial devices. The results trend can be considered of general validity, but particular values and coefficients depend on the materials used. This analysis is valid in steady-state and transient periods between load changes are not accounted for. The amount of time needed to reach steady-state and the change in power output during the transient could be studied in future work to provide additional knowledge.

The results presented in this work are noteworthy because they offer new insights on the behaviour of thermoelectric generators in conditions of constant heat input. The relationships for maximum power and efficiency, as much as the geometrical optimisation of the TEG device differ from the case of constant temperature difference, which has already been thoroughly investigated in literature. In this latter case the temperature sources across the TEG device (or after the hot and cold heat exchangers) are treated as ideal, *i.e.* capable of providing "unlimited" thermal power. However, as explained in detail in Section 2, in most waste heat recovery applications the available heat energy is limited, therefore the resulting temperatures depend significantly on the effective thermal resistance of the TEG, which depends both on its geometrical design and on the current it generates.

The results of the optimisation tool described in Section 5 are significant, because they suggest that same performance can be obtained even if using different amounts of thermoelectric material. The explanation behind this result is related to the variations of the TEG internal resistance, R_{int} (Fig. 4c), and the pellets thermal conductance, K_{legs} (Fig. 4d), with the height, h, and cross-sectional area, ω^2, of the pellets (or legs). Neglecting for this explanation the electrical and thermal contact resistances, R_{int} and K_{legs} can be written as

$$R_{int} = N \cdot R_{int,pellets} = N\rho\frac{h}{\omega^2} \quad K_{legs} = N\kappa_{legs}\frac{\omega^2}{h} \tag{11}$$

where $R_{int,pellets}$ and κ_{legs} are the internal resistance and thermal conductivity coefficient of the pellets, respectively. In Eq. (11) it is possible to maintain R_{int} and K_{legs} constant if h and ω^2 are varied by the same amount. In particular, decreasing them the volume of

thermoelectric material, $V_{TE} = N \cdot h \cdot \omega^2$ can be minimised, thus achieving significant cost savings.

As a consequence, it is possible to design the pellets geometrical parameters in order to minimise the thermoelectric material required while still producing maximum power.

Sections 4 and 5 provided the optimum parameters for the TEG pellets architecture that maximise power production for the selected value of Q_H. The obtained parameters might not maximise the power output for other thermal powers. Using these parameters with a greater Q_H will result in an excessive temperature difference established across the TEG, therefore the system designer should design for the worst case, or include means for removing excess thermal energy, *e.g.*, bypass valve in automotive exhaust systems, and find the best overall compromise: the optimum combination for N, ω, h and τ must be selected over the whole expected thermal operating range and relative to the particular system. Designing the TEG geometry as done in this work provides meaningful results because the temperature difference is calculated considering the parasitic Peltier effect when the TEG is operated.

7. Conclusions

This research study made use of a simulation tool based on steady-state equations for thermoelectric generators and experimental data to investigate behaviour and performance of TEGs with constant heat across them, and to find the pellets optimum geometrical design leading to best performance and lowest material expenditure.

This work offered a new solution to set the optimum electrical operating point in conditions of constant heat and explained how the cost associated to the thermoelectric material can be minimised, while still producing maximum power at the selected heat input condition.

This work firstly analysed the characterisation of TEG devices for constant thermal input power. It provides useful information on the performance that TEGs are likely to produce in practical applications, because in most waste heat applications at any time the maximum available heat is limited. Therefore changes in the current extracted from the TEG influence the temperature difference established across it, due to the Peltier effect. Consequently, the output power is a function of the heat power and the electrical current. Its maximum value is obtained when the load voltage approximates half of the steady-state open-circuit voltage and it is higher than half of the instantaneous open-circuit voltage.

This work also offered an insight on how the number and size of pellets, and the clearance space between them (hence the packing factor) influence the power output when considering a TEG with a fixed amount of thermal power through it. Furthermore, this work described an algorithm that calculates the best architecture of TEG pellets to maximise power production and minimise material cost for a selected constant heat condition.

The results evinced from this work can improve the design and the MPPT control of TEG devices for waste heat recovery applications, leading to enhancements in efficiency and power production. Also, they stress the importance of the Peltier effect and the need to consider not only the almost instantaneous change determined by the TEG's electrical response, but also the slower effect on the temperature difference determined by changes in the electrical load and thermal flux.

Future work will focus on experimental tests and transient simulations, applying the simulation tool described in [40], which considers all thermoelectric phenomena from the system point of view.

Acknowledgements

The authors would like to thank Dr. Gao Min of the University of Cardiff and Dr. Lourdes Ferre Llin of the University of Glasgow for the interesting discussions on this subject.

This work was partially supported by the Engineering and Physical Sciences Research Council (EPSRC) under Grant EP/K022156/1 (RCUK).

References

[1] Ramadass YK, Chandrakasan AP. A battery-less thermoelectric energy harvesting interface circuit with 35 mV startup voltage. IEEE J Solid-State Circuits 2011;46:333–41.
[2] Elefsiniotis A, Kokorakis N, Becker T, Schmid U. A thermoelectric-based energy harvesting module with extended operational temperature range for powering autonomous wireless sensor nodes in aircraft. Sens Actuat A: Phys 2014;206:159–64.
[3] Kinsella C, O'Shaughnessy S, Deasy M, Duffy M, Robinson aJ. Battery charging considerations in small scale electricity generation from a thermoelectric module. Appl Energy 2014;114:80–90.
[4] Crane D, LaGrandeur J, Jovovic V, Ranalli M, Adldinger M, Poliquin E, et al. TEG on-vehicle performance and model validation and what it means for further TEG development. J Electron Mater 2012.
[5] Risse S, Zellbeck H. Close-coupled exhaust gas energy recovery in a gasoline engine. Res Therm Manage 2013;74:54–61.
[6] Champier D, Bedecarrats JP, Kousksou T, Rivaletto M, Strub F, Pignolet P. Study of a TE (thermoelectric) generator incorporated in a multifunction wood stove. Energy 2011;36:1518–26.
[7] O'Shaughnessy S, Deasy M, Kinsella C, Doyle J, Robinson A. Small scale electricity generation from a portable biomass cookstove: prototype design and preliminary results. Appl Energy 2013;102:374–85.
[8] Chen M, Lund H, Rosendahl La, Condra TJ. Energy efficiency analysis and impact evaluation of the application of thermoelectric power cycle to todays CHP systems. Appl Energy 2010;87:1231–8.
[9] Qiu K, Hayden ACS. Development of a novel cascading TPV and TE power generation system. Appl Energy 2012;91:304–8.
[10] Sark WV. Feasibility of photovoltaic thermoelectric hybrid modules. Appl Energy 2011;88:2785–90.
[11] Kaibe H, Makino K, Kajihara T, Fujimoto S, Hachiuma H. Thermoelectric generating system attached to a carburizing furnace at Komatsu Ltd., Awazu Plant. In: 9th European conference on thermoelectrics, 2011 (ECT'11), p. 524–7.
[12] Suter C, Jovanovic Z, Steinfeld A. A 1;kWe thermoelectric stack for geothermal power generation: modeling and geometrical optimization. Appl Energy 2012;99:379–85.
[13] Patyk A. Thermoelectric generators for efficiency improvement of power generation by motor generators: environmental and economic perspectives. Appl Energy 2013;102:1448–57.
[14] Rowe D, Min G. Evaluation of thermoelectric modules for power generation. J Power Sources 1998;73:193–8.
[15] Lineykin S, Ben-Yaakov S. Modeling and analysis of thermoelectric modules. IEEE Trans Ind Appl 2007;43:505–12.
[16] Laird I, Lovatt H, Savvides N, Lu D, Agelidis VG. Comparative study of maximum power point tracking algorithms for thermoelectric generators. In: Australasian universities power engineering conference, 2008 (AUPEC'08).
[17] Min G, Yatim NM. Variable thermal resistor based on self-powered Peltier effect. J Phys D: Appl Phys 2008;41:222001.
[18] Kumar S, Heister SD, Xu X, Salvador JR, Meisner GP. Thermoelectric generators for automotive waste heat recovery systems Part I: Numerical modeling and baseline model analysis. J Electron Mater 2013;42:665–74.
[19] Chen L, Cao D, Yi H, Peng FZ. Modeling and power conditioning for thermoelectric generation. In: Power electronics specialists conference. IEEE; 2008. p. 1098–103.
[20] Mayer P, Ram R. Optimization of heat sinklimited thermoelectric generators. Nanoscale Microscale Thermophys Eng 2006;10:143–55.
[21] Gomez M, Reid R, Ohara B, Lee H. Influence of electrical current variance and thermal resistances on optimum working conditions and geometry for thermoelectric energy harvesting. J Appl Phys 2013:0–8.
[22] Montecucco A, Buckle JR, Knox AR. Solution to the 1-D unsteady heat conduction equation with internal Joule heat generation for thermoelectric devices. Appl Therm Eng 2012;35:177–84.
[23] Yazawa K, Shakouri A. Cost-efficiency trade-off and the design of thermoelectric power generators. Environ Sci Technol 2011;45:7548–53.
[24] McCarty R. Thermoelectric power generator design for maximum power: its all about ZT. J Electron Mater 2012;42:1504–8.
[25] Nemir D, Beck J. On the significance of the thermoelectric figure of merit Z. J Electron Mater 2010;39:1897–901.
[26] Apertet Y, Ouerdane H, Glavatskaya O, Goupil C, Lecoeur P. Optimal working conditions for thermoelectric generators with realistic thermal coupling. EPL (Europhys Lett) 2012;97:28001.
[27] Wang Y, Dai C, Wang S. Theoretical analysis of a thermoelectric generator using exhaust gas of vehicles as heat source. Appl Energy 2013;112:1171–80.

[28] Rezania A, Rosendahl L, Yin H. Parametric optimization of thermoelectric elements footprint for maximum power generation. J Power Sources 2014;255:151–6.
[29] Lee H. Optimal design of thermoelectric devices with dimensional analysis. Appl Energy 2013;106:79–88.
[30] Jang J-Y, Tsai Y-C. Optimization of thermoelectric generator module spacing and spreader thickness used in a waste heat recovery system. Appl Therm Eng 2013;51:677–89.
[31] Favarel C, Bédécarrats J-P, Kousksou T, Champier D. Numerical optimization of the occupancy rate of thermoelectric generators to produce the highest electrical power. Energy 2014;68:104–16.
[32] Kajihara T. Study of thermoelectric generation unit for radiant waste heat. In: 12th European conference on thermoelectrics, 2014 (ECT'14).
[33] Fraisse G, Ramousse J, Sgorlon D, Goupil C. Comparison of different modeling approaches for thermoelectric elements. Energy Convers Manage 2013;65:351–6.
[34] Sandoz-Rosado EJ, Weinstein SJ, Stevens RJ. On the Thomson effect in thermoelectric power devices. Int J Therm Sci 2013;66:1–7.
[35] Montecucco A, Siviter J, Knox AR. The effect of temperature mismatch on thermoelectric generators electrically connected in series and parallel. Appl Energy 2014;123:47–54.
[36] Montecucco A, Knox AR. Maximum power point tracking converter based on the open-circuit voltage method for thermoelectric generators. IEEE Trans Power Electron 2015;30:828–39.
[37] Kim R-Y, Lai J-S. A seamless mode transfer maximum power point tracking controller for thermoelectric generator applications. IEEE Trans Power Electron 2008;23:2310–8.
[38] Kim R-Y, Lai J-S, York B, Koran A. Analysis and design of maximum power point tracking scheme for thermoelectric battery energy storage system. IEEE Trans Ind Electron 2009;56:3709–16.
[39] Min G. Thermoelectric energy harvesting. In: Energy harvesting for autonomous systems, vol. 413–414, Artech House; 2010, p. 135–57.
[40] Montecucco A, Knox AR. Accurate simulation of thermoelectric power generating systems. Appl Energy 2014;118:166–72.